

**Kinetic energy of fermionic systems**V. Zampronio<sup>1,\*</sup> and S. A. Vitiello<sup>1,2,†</sup><sup>1</sup>*Instituto de Física Gleb Wataghin, University of Campinas-UNICAMP, 13083-859 Campinas, São Paulo, Brazil*<sup>2</sup>*CENAPAD-SP, University of Campinas-UNICAMP, 13083-889 Campinas, São Paulo, Brazil*

(Received 26 April 2018; revised manuscript received 7 January 2019; published 25 January 2019)

The kinetic energy of a system made from normal  $^3\text{He}$  liquid is estimated and shows that progress has been made in resolving a long-standing disagreement with most experimental values of this quantity. In general, in the investigation of systems formed from strongly correlated fermions, the disagreement between experimental and “exact” theoretical values of the kinetic energy is a matter of concern. For these systems, difficulties are not only due to the Fermi-Dirac statistics they must obey, but also are due to the configurations that are used in estimations of quantities that do not commute with the Hamiltonian. We are able to improve the sampling of configurations and to avoid most of the bias from variational theories. Bias analysis and unbiased estimates of quantities that do not commute with the system Hamiltonian are also easily made.

DOI: [10.1103/PhysRevB.99.045145](https://doi.org/10.1103/PhysRevB.99.045145)**I. INTRODUCTION**

Fermions, one of the building blocks of matter, are of immense interest in a variety of scientific fields, ranging from many-body studies and optical traps with few atoms to particle physics. In condensed matter, ultracold gases can generate “artificial” solids that can be used as quantum simulators as imagined by Feynman [1]. The possibility of tuning the interparticle potential of fermionic gases via Feshbach resonance is of capital importance in the study of converting atoms into dimers and Cooper pairs [2]. The interplay between experimental results and quantum Monte Carlo methods [3–13] shows how important these methods are as a tool to clarify properties of strongly correlated many-body systems.

Kinetic energy is a fundamental property of quantum many-body systems. It is the relative importance of this property compared to the interactions in the system that determines its overall behavior. The balance between kinetic and potential energies can promote the formation of exotic phases in ultracold dipolar quantum gases [14]. From the theoretical point of view, what determines the most suitable treatment for a system emerges from a comparison between an interacting Hamiltonian and a free one.

Repulsive strongly interacting fermionic gases and the question of ferromagnetic instabilities [15–18] are relevant for a Stoner-like phase transition with a magnetic behavior arising from the interaction between itinerant fermions. The kinetic energy at the ferromagnetic transition obtained in experiment [18] and theory [17] does not even show qualitative agreement. The ubiquitous systems formed from helium atoms used as the workbench for many-body theories also have a quantitative disagreement regarding the kinetic energy of experimental and theoretical values of  $^3\text{He}$  [19,20].

We may note that these measurements, using deep inelastic neutron scattering, are challenging experiments because the absorption cross section for thermal neutrons is about three orders of magnitude higher than for inelastic scattering.

Quantum Monte Carlo (QMC) methods at temperature  $T = 0$  are, in principle, able to give “exact” results, subjected only to statistical uncertainties for quantities that commute with the system Hamiltonian. For quantities without this property, approximations need to be considered. For systems made from Fermi particles, the situation is even more delicate because of the antisymmetrical character of the Fermi-Dirac statistics that need to be satisfied by these systems. This is the origin of the so-called sign problem that prevents convergence of the calculations. In general, it belongs to the computational complexity class of nondeterministic polynomial hard [21] problems. Difficulties that QMC methods have with the sign problem are not exclusive in the upper bound estimations of the total energy; they can almost certainly reinforce discrepancies between experimental and theoretical values of properties associated with operators that do not commute with the system Hamiltonian.

In this paper, we show how to mitigate difficulties associated with the sign problem, how to improve the sampling of the configuration space, and how to avoid approximations in the estimation of noncommuting quantities with the Hamiltonian by extending the variational path-integral [(VPI), also known as the path-integral ground-state] method [22,23] to strongly correlated many-fermion systems. To demonstrate the strength and simplicity of our approach, we use one of the most studied and simplest strongly correlated fermionic systems, liquid  $^3\text{He}$  in which there are still controversies about the kinetic-energy value. Additionally, at least for these systems, we also show that in exact QMC methods, contrary to common belief, it is not always true that estimations of quantities associated with operators that do not commute with the Hamiltonian are consistently benefited when the accuracy of a trial state is increased.

\*viniciuz@ifi.unicamp.br

†vitiello@ifi.unicamp.br

## II. METHODS

The VPI method in its original formulation is well established for the investigation of a variety of bosonic systems [24–29] at zero temperature. This method projects the ground state from trial functions  $\Psi_T$  using the density-matrix  $\rho(\beta) = \exp(-\beta H)$ , where  $H$  is the system Hamiltonian. The state  $|\Psi(\beta)\rangle = \rho(\beta)|\Psi_T\rangle$  converges exponentially to the ground-state  $|\Psi_0\rangle$  as  $\beta$  increases. An exact value of any property can be estimated by constructing a string with convolution of simple forms of the density operators with trial states at its extremities. A property associated with any operator  $\mathcal{O}$  can be estimated by its application at the middle of the string for large enough values of  $\beta$  able to assure a converged value of this quantity,

$$O(2\beta) \propto \langle \Psi(\beta) | \mathcal{O} | \Psi(\beta) \rangle = \langle \Psi_T | \rho(\beta) \mathcal{O}_L \rho(\beta) | \Psi_T \rangle, \quad (1)$$

where  $O_L(R_i) = \mathcal{O} \rho(R_i, R_{i+1}, \tau) / \rho(R_i, R_{i+1}, \tau)$  is a local value estimator for a particular value  $\tau$  (usually  $\tau \ll \beta$ ),  $R_i$  is a configuration of the system, and  $\rho(R_i, R_{i+1}, \tau) = \langle R_i | \rho(\tau) | R_{i+1} \rangle$  is a matrix element of  $\rho(\tau)$  in the coordinate representation.

To be more specific, ground-state properties are estimated by constructing estimators and applying them to the state  $|\Psi(\beta)\rangle = \rho(\beta)|\Psi_T\rangle$ . The matrix element  $\rho(R, R', \beta)$  propagates the trial function  $\Psi_T(R')$  to  $\Psi(R, \beta) = \langle R | \Psi(\beta) \rangle$  in a “time”  $\beta$  [22]. It is written as the exponential of the action integrated over all paths. The integration can be made by factorizing  $\rho(\beta)$  into the product of  $M$  projectors  $\rho(\tau)$ ,  $\tau = \beta/M$ , and using the convolution property,

$$\rho(R, R', \beta) = \int dR_1 \cdots dR_{M-1} \rho(R, R_1, \tau) \times \rho(R_1, R_2, \tau) \cdots \rho(R_{M-1}, R', \tau). \quad (2)$$

The intermediary configurations or beads  $R_n$ ,  $n = 1, \dots, M-1$ , can be seen as the set of atomic coordinates at time  $t = n\tau$ . The beads stand for a sort of discretization of the path from  $R$  to  $R'$  in a time  $\beta$ . Therefore the integration of Eq. (2) converges to the integration over all paths if  $\tau$  is small enough. Any error introduced by this approximation can, in general, be made smaller than the statistical uncertainties of the Monte Carlo method.

In the usual path-integral Monte Carlo calculations we find closed polymers. Whereas in the VPI method, the polymers are opened and a trial function is attached to their ends. We call these polymers strings. Configurations  $R_i$  of  $\rho(R, R', \beta)$  at the middle of long enough strings allow one to estimate any quantity without further approximation, even if its expected values are associated with operators that do not commute with the Hamiltonian.

If a given property is associated with an operator  $\mathcal{O}$ , an estimate of this quantity can be written as

$$O \propto \langle \Psi(\beta) | \mathcal{O} | \Psi(\beta) \rangle = \langle \Psi_T | \rho(\beta) \mathcal{O} \rho(\beta) | \Psi_T \rangle. \quad (3)$$

The last expression can also be written as

$$O = \int dR_1 \cdots dR_{2M+1} P(R_1, \dots, R_{2M+1}) O_L, \quad (4)$$

in terms of the probability distribution function  $P$  of a given path,

$$P(R_1, \dots, R_{2M+1}) \propto \Psi_T(R_1) \rho(R_1, R_2, \tau) \cdots \times \rho(R_{2M}, R_{2M+1}, \tau) \Psi_T(R_{2M+1}). \quad (5)$$

In Eq. (4),  $O_L(R_i, R_{i+1}) = \mathcal{O} \rho(R_i, R_{i+1}, \tau) / \rho(R_i, R_{i+1}, \tau)$  is the local value of operator  $\mathcal{O}$  in the coordinate representation.

For the estimation of the total and kinetic energies, it is still possible to use the so-called thermodynamic estimators. They are constructed by taking derivatives of  $\rho(\beta)$  regarding  $\beta$  and mass  $m$ , respectively.

## III. FERMIONIC SYSTEMS

More importantly, the application of the VPI method to strongly correlated Fermi systems is not difficult if antisymmetrical trial functions  $\Psi_T(R)$  are used at the end of the string. The matrix element  $\rho(R, R', \beta)$  does not explicitly need to be antisymmetrical under the permutation of any pair of particles of configuration  $R$ . It is enough to incorporate the minus sign arising from odd permutations of  $\rho(R, R', \beta)$  into  $\Psi_T(R)$  since

$$\rho(R, R', \beta) \Psi_T(R') = (-1)^{n_p} \rho(R, \mathcal{P}R', \beta) \Psi_T(R') = \rho(R, \mathcal{P}R', \beta) \Psi_T(\mathcal{P}R'), \quad (6)$$

where  $\mathcal{P}$  is a permutation operator that changes the coordinates of  $n_p$  particles in a given configuration. We observe that, after integration in  $R'$ , all permutations will have the same result and therefore, in contrast to other Monte Carlo calculations, these permutations do not need to be explicitly considered. The above proof allows us to treat the sign problem in a much less stringent manner than other Monte Carlo methods. It is enough to reject samples where the product of  $\Psi_T(R_e) \Psi_T(R'_e)$  at the extremities of the string changes sign. This is a fixed-node approximation that has more degrees of freedom than the restriction  $\Psi_T(R) > 0$  imposed when one applies an importance function transformation to sample  $\Psi_0(R) \Psi_T(R)$  in iterative Monte Carlo methods. In each of these iterations, configurations best known in the literature as walkers evolve in time, and the fixed-node restrictions are imposed in the sampling of each and every iteration. In the VPI method, this would be equivalent to performing the fixed-node approximation in the sampling of all internal beads instead of considering it only at the extremities of the string. We believe that the extra degrees of freedom allowed by this implementation of the fixed-node approximation improves the exploration of the configuration space especially in regions where the nodal structure of  $\Psi_T(R)$  is not identical to that of the ground state.

To project the ground state from a trial function  $\Psi_T$ , we carried out calculations using two distinct approximations to  $\rho(R, R', \tau)$  in Eq. (2). We have experimented with the primitive approximation [22], which is a second order in  $\tau$  and a fourth-order approximation in  $\tau$ , from Refs. [30,31]. The choice of either of these approximations did not affect our results.

#### IV. TRIAL WAVE FUNCTIONS AT THE EXTREMITIES

We chose two distinct trial wave functions to project out the ground state. The simplest function we have used at the extremities was the Jastrow-Slater (JS) wave function,

$$\Psi_T(R) = \prod_{i,j} e^{-(1/2)u(r_{ij})} \det_{\uparrow}(e^{i\mathbf{k}_i \cdot \mathbf{r}_m}) \det_{\downarrow}(e^{i\mathbf{k}_i \cdot \mathbf{r}_n}), \quad (7)$$

where  $u(r) = (b/r)^5$ . The nodal structure of this wave function was improved by adding backflow (BF) correlations in the Slater determinant [32,33]. These correlations are introduced by a change in the particle coordinates  $\mathbf{r}_i \rightarrow \mathbf{r}_i + \sum_{j \neq i} \eta(r_{ij})(\mathbf{r}_i - \mathbf{r}_j)$  of the Slater determinant, where

$$\eta(r) = \lambda_B e^{-[(r-s_B)/w_B]^2} + \frac{\lambda'_B}{r^3}, \quad (8)$$

and  $\lambda_B$ ,  $s_B$ ,  $w_B$ , and  $\lambda'_B$  are parameters. Three-body (T) correlations [32,33] were also introduced in the symmetric part of  $\Psi_T(R)$ ,

$$\exp \left[ -\frac{1}{2} \sum_{i < j} \tilde{u}(|\mathbf{r}_i - \mathbf{r}_j|) - \frac{\lambda_T}{4} \sum_l \mathbf{G}(l) \cdot \mathbf{G}(l) \right], \quad (9)$$

where  $\mathbf{G}(l) = \sum_{i \neq j} \xi(r_{ij}) \mathbf{r}_{ij}$ ,  $\xi(r) = \exp[-(r-s_T)/(w_T)]^2$ , and  $s_T$ ,  $w_T$  are parameters. The pseudopotential  $\tilde{u}(r) = u(r) - \lambda_T \xi^2(r) r^2$  cancels two-body factors arising  $\mathbf{G}(l) \cdot \mathbf{G}(l)$ . We refer to this improved wave function as JS + BF + T.

#### V. RESULTS AND DISCUSSIONS

We applied the VPI method to study a system of 54 atoms of  $^3\text{He}$  at the equilibrium density of  $0.0163 \text{ \AA}^{-3}$  in a cubic cell with periodic boundary conditions described by the Hamiltonian,

$$H = \frac{1}{2m} \sum_{i=1}^N \nabla_i^2 + \sum_{i < j}^N v(r_{ij}), \quad (10)$$

where  $m$  is the  $^3\text{He}$  mass and  $v(r)$  is a very accurate pairwise potential [34].

We experimented our fixed-node approximation with distinct trial wave functions that have different degrees of overlapping with the ground state. The simplest one is known as the JS wave function. It describes a fermion fluid by means of a symmetrical two-body correlation factor multiplied by one determinant of plane waves for the spin-up atoms and another for the spin-down atoms. These atoms fill the Fermi sphere representing the unpolarized state of an ideal gas. A more elaborate function, JS + BF + T, included explicit T correlations and an improved description of the nodal structure of the ideal gas by introducing the so-called BF correlations.

The purpose of using two different trial functions at the ends of the string (JS-JS or JS + BF + T-JS + BF + T) is twofold. First, we demonstrate that the reasoning leading to Eq. (6) is not affected by any numerical artifact. Second, we show that an improved trial function accelerates convergence to the exact ground state especially if it has a more accurate nodal structure. We have evaluated the total energy  $H(2\beta)$  as a function of  $\beta$  with the results displayed in Fig. 1.

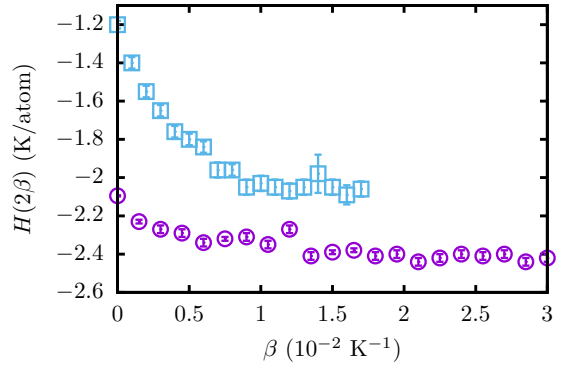


FIG. 1. Total energy  $H(2\beta)$  as a function of  $\beta$ . The points at  $\beta = 0$  correspond to variational energies. Squares represent the calculations with the JS trial function, and circles stand for calculations using the JS + BF + T function.

As  $\beta$  increases, the energy decreases, almost exponentially, creating a sequence of upper bound values to the ground-state energy until a converged value is reached. It is clear that the converged value obtained using a state projected from the more elaborate wave function is considerably lower than the one projected from the JS wave function. This last function has a poorer nodal structure; which is considerably improved by BF correlations as is well known. Of course, the true ground-state energy itself would only be achieved if the nodal structure of  $\Psi_T(R)$  is identical to the exact one.

A constant straight line was fitted starting at  $\beta \geq 1.5 \times 10^{-2} \text{ K}^{-1}$  to converged values of the energy (Fig. 1) associated with the string containing the JS + BF + T function at its ends. From this fit, the total energy was estimated as  $-2.41 \pm 0.01 \text{ K/atom}$ , a very good upper bound to the experimental datum  $-2.47 \pm 0.01 \text{ K/atom}$  [35]. From now on, all results we report are exclusively obtained with this wave function.

For converged values of the kinetic energy as a function of  $\beta$ , a constant straight line was fitted. The ground-state kinetic energy obtained is  $10.16 \pm 0.05 \text{ K/atom}$ . In Fig. 2, we plotted this value together with experimental data from the literature for liquid  $^3\text{He}$  at equilibrium density. Most of the experimental data lie in a range from 8 to 11 K/atom, which is in excellent agreement with our estimates. We excluded from

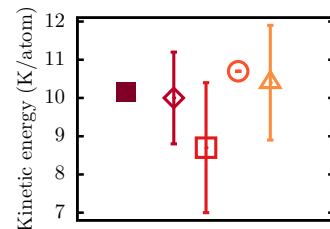


FIG. 2. Comparison of our results for the kinetic energy of  $^3\text{He}$  at the equilibrium density and experimental data from the literature. The symbols were horizontally displaced for the sake of clarity. The full square stands for our calculation; this symbol size is larger than the statistical uncertainty. The experimental data are plotted with empty symbols: square [39], circle [40], triangle [41], and rhombus [42].

TABLE I. Fitted values of the kinetic and potential energies in units of K/atom to converged values of these quantities obtained with the local and thermodynamic ( $\mathcal{T}$ ) estimators. Configurations are projected from the JS + BF + T wave function. The result in the last line was obtained using values from both estimators.

Estimator	Kinetic energy	Potential energy
Local	$10.19 \pm 0.07$	$-12.75 \pm 0.01$
$\mathcal{T}$	$10.14 \pm 0.07$	$-12.75 \pm 0.01$
Local + $\mathcal{T}$	$10.16 \pm 0.05$	$-12.75 \pm 0.01$

Fig. 2 a datum from Ref. [20] because its value and error bars lie between previous theoretical results and those of other experiments, which allows agreement with both sets of values. Former computed values of the kinetic energy are in the range of 12 to 13 K/atom [33,36–38].

For the sake of completeness, we report in Table I the estimates of kinetic energy of liquid  $^3\text{He}$  calculated using the local and the thermodynamics estimators. The adopted value of the kinetic energy  $10.16 \pm 0.05$  K/atom is obtained considering both estimators.

A possible source of disagreement between our result and those from the literature can be attributed to the fact that they need to rely on an approximation that might introduce bias into the final answers. This approximation consists in computing the desired value through the extrapolated estimator  $O_{\text{extr}} \approx 2O_{\text{mix}} - O_{\text{var}}$ , where  $O_{\text{var}}$  is the usual variational estimate of the expected value of  $\mathcal{O}$  and  $O_{\text{mix}}$  is the commonly mixed estimate of iterative Monte Carlo projector methods. The estimator of  $O_{\text{mix}}$  is a special case of our local estimator for a large enough  $\beta$ ,

$$O_{\text{mix}} = \frac{\langle \Psi_T | \mathcal{O} | \Psi_0 \rangle}{\langle \Psi_T | \Psi_0 \rangle} = \frac{\langle \Psi_T | \mathcal{O} | \Psi(2\beta) \rangle}{\langle \Psi_T | \Psi(2\beta) \rangle}. \quad (11)$$

If  $\mathcal{O}$  is the system Hamiltonian, the above estimator gives, at any intermediate configuration  $R_i$  of a long enough string, the exact value of the ground-state energy. This is also true for any quantity that commutes with the system Hamiltonian.

For the purposes of comparison with values from the literature, it is useful and straightforward to use the extrapolation technique in the context of the VPI method. The extrapolation approximation performed with  $O_{\text{extr}}$  is correct up to the second order in the difference between the trial state and the ground state. We obtained an extrapolated kinetic energy of  $11.27 \pm 0.01$  K/atom. This value is not in agreement with our exact estimate nor with extrapolated values from the literature. Nevertheless, our exact result is closer to this last value than those from the literature. This fact might suggest that our method samples the configuration space in a more efficient manner than other approaches. Moreover, since we note that extrapolations give more consistent results when used with bosonic systems [43], this also might reinforce a view that we have a more accurate treatment of the fermionic sign problem. On that point, we also note that extrapolations are somehow more problematic in fermionic systems. This approximation is used to cancel the first-order contributions in the difference between the trial state and the ground state. To this aim, a linear combination of the mixed and variational estimates is

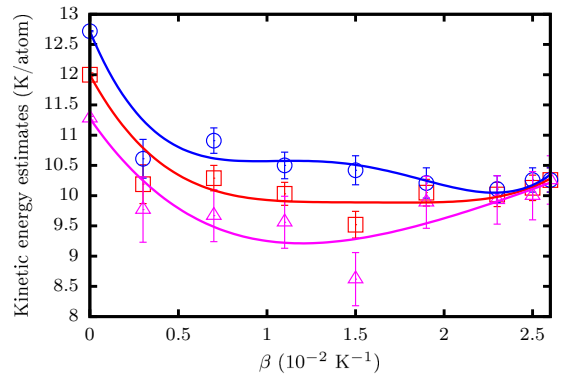


FIG. 3. Variational ( $\circ$ ), mixed ( $\square$ ), and extrapolated ( $\triangle$ ) estimates for the kinetic energy obtained from the improved trial state  $|\Psi(\beta)\rangle$  as a function of  $\beta$ . The full lines are fourth-order polynomial fits of the results.

performed. However, in fermionic systems, restrictions on the integration of the mixed estimate are imposed due to the sign problem, whereas those same restrictions are not made for the variational estimate since in this case one samples the square of the trial wave function. Thus, the cancellation intended is not complete.

Related to these questions, we have investigated if extrapolated approximations are benefited by improvements of the trial function  $\Psi_T(R)$ . We calculated mixed  $\langle \Psi(\beta) | \mathcal{O} | \Psi_0 \rangle$  and variational  $\langle \Psi(\beta) | \mathcal{O} | \Psi(\beta) \rangle$  estimates for increasing values of  $\beta$ . The results for the kinetic energy are shown in Fig. 3 where it becomes clear that extrapolations converge to the exact result only when  $|\Psi(\beta)\rangle$  tends to the system ground state.

As another property that does not commute with the system Hamiltonian, we have estimated the total radial distribution function and its spin-resolved components for atoms with

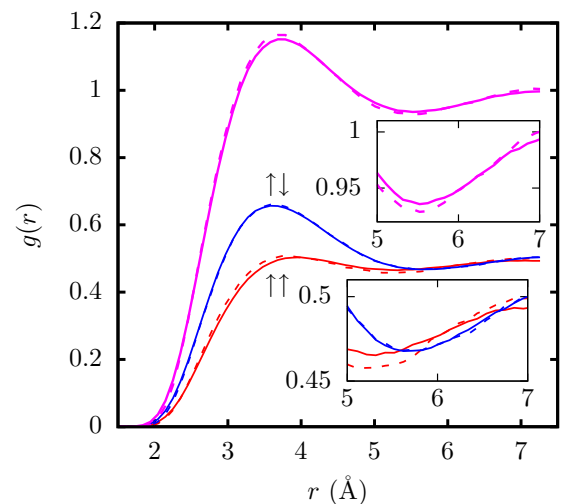


FIG. 4. Exact (solid line) and extrapolated (dashed line) radial distribution functions and their spin-resolved components, parallel ( $\uparrow\uparrow$ ), and antiparallel ( $\uparrow\downarrow$ ) as a function of the radial distance between pairs for liquid  $^3\text{He}$  at equilibrium density. The insets show the details of the results near the first minimum.



parallel and antiparallel spins,

$$g(r) = \frac{1}{\text{Vol}} \left\langle \sum_{i < j} \delta(r - r_{ij}) \right\rangle, \quad (12)$$

where Vol is the volume of the simulation cell. The results can be seen in Fig. 4. As expected, the antiparallel spin curve has a more pronounced peak because of the Pauli exclusion principle. In the same figure, for comparison, we present extrapolated estimates that show differences from our results.

## VI. CONCLUSIONS

The VPI approach we have presented to investigate strongly correlated Fermi systems is robust and reliable. It allows a more efficient exploration of the configuration space

and improved results can be obtained. Any quantity associated with operators that do or do not commute with the Hamiltonian can be readily obtained by unbiased estimators. The potentiality of this method was demonstrated by calculations of the ground-state kinetic energy of liquid  $^3\text{He}$  leading finally to results that are in agreement with most of its experimental values.

## ACKNOWLEDGMENTS

The authors acknowledge financial support from the Brazilian agencies Fundação de Amparo à Pesquisa do Estado de São Paulo (FAPESP) and Conselho Nacional de Desenvolvimento Científico e Tecnológico (CNPq). Part of the computations were performed at the Centro Nacional de Processamento de Alto Desempenho em São Paulo (CENAPAD-SP).

- 
- [1] C. Gross and I. Bloch, *Science* **357**, 995 (2017).
- [2] V. Barbé, A. Ciamei, B. Pasquiou, L. Reichsöllner, F. Schreck, P. S. Žuchowski, and J. M. Hutson, *Nat. Phys.* **14**, 881 (2018).
- [3] J. Carlson, S. Gandolfi, U. van Kolck, and S. A. Vitiello, *Phys. Rev. Lett.* **119**, 223002 (2017).
- [4] S. Laurent, M. Pierce, M. Delehay, T. Yefsah, F. Chevy, and C. Salomon, *Phys. Rev. Lett.* **118**, 103403 (2017).
- [5] M. Boll, T. A. Hilker, G. Salomon, A. Omran, J. Nespolo, L. Pollet, I. Bloch, and C. Gross, *Science* **353**, 1257 (2016).
- [6] W. Weimer, K. Morgener, V. P. Singh, J. Siegl, K. Hueck, N. Luick, L. Mathey, and H. Moritz, *Phys. Rev. Lett.* **114**, 095301 (2015).
- [7] M. J. H. Ku, A. T. Sommer, L. W. Cheuk, and M. W. Zwierlein, *Science* **335**, 563 (2012).
- [8] A. Bulgac, Y.-L. Luo, P. Magierski, K. J. Roche, and Y. Yu, *Science* **332**, 1288 (2011).
- [9] R. Pessoa, S. A. Vitiello, and M. de Koning, *Phys. Rev. Lett.* **104**, 085301 (2010).
- [10] S. Nascimbène, N. Navon, K. J. Jiang, F. Chevy, and C. Salomon, *Nature (London)* **463**, 1057 (2010).
- [11] N. Navon, S. Nascimbène, F. Chevy, and C. Salomon, *Science* **328**, 729 (2010).
- [12] H. Hu, P. D. Drummond, and X.-J. Liu, *Nat. Phys.* **3**, 469 (2007).
- [13] G. B. Partridge, *Science* **311**, 503 (2006).
- [14] L. Chomaz, R. M. W. van Bijnen, D. Petter, G. Faraoni, S. Baier, J. H. Becher, M. J. Mark, F. Wächtler, L. Santos, and F. Ferlaino, *Nat. Phys.* **14**, 442 (2018).
- [15] G. Valtolina, F. Scazza, A. Amico, A. Burchianti, A. Recati, T. Enss, M. Inguscio, M. Zaccanti, and G. Roati, *Nat. Phys.* **13**, 704 (2017).
- [16] Z. Sun and Q. Gu, *Sci. Rep.* **6**, 31776 (2016).
- [17] S.-Y. Chang, M. Randeria, and N. Trivedi, *Proc. Natl. Acad. Sci. U.S.A.* **108**, 51 (2011).
- [18] G.-B. Jo, Y.-R. Lee, J.-H. Choi, C. A. Christensen, T. H. Kim, J. H. Thywissen, D. E. Pritchard, and W. Ketterle, *Science* **325**, 1521 (2009).
- [19] M. Boninsegni, *J. Chem. Phys.* **148**, 102308 (2018).
- [20] M. S. Bryan, T. R. Prisk, R. T. Azuah, W. G. Stirling, and P. E. Sokol, *Europhys. Lett.* **115**, 66001 (2016).
- [21] M. Troyer and U.-J. Wiese, *Phys. Rev. Lett.* **94**, 170201 (2005).
- [22] D. M. Ceperley, *Rev. Mod. Phys.* **67**, 279 (1995).
- [23] S. Vitiello, K. Runge, and M. H. Kalos, *Phys. Rev. Lett.* **60**, 1970 (1988).
- [24] C. M. Herdman, P.-N. Roy, R. G. Melko, and A. D. Maestro, *Nat. Phys.* **13**, 556 (2017).
- [25] S. Rossotti, M. Teruzzi, D. Pini, D. E. Galli, and G. Bertaina, *Phys. Rev. Lett.* **119**, 215301 (2017).
- [26] R. Bombin, J. Boronat, and F. Mazzanti, *Phys. Rev. Lett.* **119**, 250402 (2017).
- [27] G. Bertaina, M. Motta, M. Rossi, E. Vitali, and D. E. Galli, *Phys. Rev. Lett.* **116**, 135302 (2016).
- [28] A. Macia, J. Sánchez-Baena, J. Boronat, and F. Mazzanti, *Phys. Rev. Lett.* **117**, 205301 (2016).
- [29] B. P. Abolins, R. E. Zillich, and K. B. Whaley, *J. Chem. Phys.* **148**, 102338 (2018).
- [30] J. E. Cuervo, P.-N. Roy, and M. Boninsegni, *J. Chem. Phys.* **122**, 114504 (2005).
- [31] M. Rossi, M. Nava, L. Reatto, and D. E. Galli, *J. Chem. Phys.* **131**, 154108 (2009).
- [32] K. E. Schmidt, M. A. Lee, M. H. Kalos, and G. V. Chester, *Phys. Rev. Lett.* **47**, 807 (1981).
- [33] R. M. Panoff and J. Carlson, *Phys. Rev. Lett.* **62**, 1130 (1989).
- [34] R. A. Aziz, A. R. Janzen, and M. R. Moldover, *Phys. Rev. Lett.* **74**, 1586 (1995).
- [35] T. R. Roberts, R. H. Sherman, and S. G. Sydorik, *J. Res. Natl. Bur. Stand.* **68A**, 567 (1964).
- [36] F. Mazzanti, A. Polls, J. Boronat, and J. Casulleras, *Phys. Rev. Lett.* **92**, 085301 (2004).
- [37] J. Casulleras and J. Boronat, *Phys. Rev. Lett.* **84**, 3121 (2000).
- [38] S. Moroni, G. Senatore, and S. Fantoni, *Phys. Rev. B* **55**, 1040 (1997).
- [39] P. E. Sokol, K. Sköld, D. L. Price, and R. Kleb, *Phys. Rev. Lett.* **55**, 2368 (1985).
- [40] H. A. Mook, *Phys. Rev. Lett.* **55**, 2452 (1985).
- [41] R. T. Azuah, W. G. Stirling, K. Guckelsberger, R. Scherm, S. M. Bennington, M. L. Yates, and A. D. Taylor, *J. Low Temp. Phys.* **101**, 951 (1995).
- [42] R. M. Dimeo, P. E. Sokol, R. T. Azuah, S. M. Bennington, W. G. Stirling, and K. Guckelsberger, *Physica B* **241–243**, 952 (1998).
- [43] A. Sarsa, K. E. Schmidt, and W. R. Magro, *J. Chem. Phys.* **113**, 1366 (2000).